Annales Geophysicae, 23, 3633–3643, 2005
SRef-ID: 1432-0576/ag/2005-23-3633

Annales Geophysicae

The effect of electron bite-outs on artificial electron heating and the PMSE overshoot

M. Kassa[1], **O. Havnes**[1,2], **and E. Belova**[3]

[1]Department of Physics, University of Tromsø, Norway
[2]UNIS, Longyearbyen, Svalbard, Norway
[3]Swedish Institute of Space Physics, IRF, Kiruna, Sweden

Received: 6 April 2005 – Revised: 20 September 2005 – Accepted: 21 November 2005 – Published: 23 December 2005

Abstract. We have considered the effect that a local reduction in the electron density (an electron bite-out), caused by electron absorption on to dust particles, can have on the artificial electron heating in the height region between 80 to 90 km, where noctilucent clouds (NLC) and the radar phenomenon PMSE (Polar Mesospheric Summer Echoes) are observed. With an electron density profile without bite-outs, the heated electron temperature $T_{e,\mathrm{hot}}$ will generally decrease smoothly with height in the PMSE region or there may be no significant heating effect present. Within a bite-out $T_{e,\mathrm{hot}}$ will decrease less rapidly and can even increase slightly with height if the bite-out is strong. We have looked at recent observations of PMSE which are affected by artificial electron heating, with a heater cycling producing the new overshoot effect. According to the theory for the PMSE overshoot the fractional increase in electron temperature $T_{e,\mathrm{hot}}/T_i$, where T_i is the unaffected ion temperature = neutral temperature, can be found from the reduction in PMSE intensity as the heater is switched on. We have looked at results from four days of observations with the EISCAT VHF radar (224 MHz), together with the EISCAT heating facility. We find support for the PMSE overshoot and heating model from a sequence of observations during one of the days where the heater transmitter power is varied from cycle to cycle and where the calculated $T_{e,\mathrm{hot}}/T_i$ is found to vary in proportion to the transmitter power. We also looked for signatures of electron bite-outs by examining the variation of $T_{e,\mathrm{hot}}/T_i$ with height for the three other days. We find that the height variation of $T_{e,\mathrm{hot}}/T_i$ is very different on the three days. On one of the days we see typically that this ratio can increase with height, showing the presence of a bite-out, while on the next day the heating factor mainly decreases with height, indicating that the fractional amount of dust is low, so that the electron density is hardly affected by it. On the third day there is little heating effect on the PMSE layer. This is probably due to a sufficiently high electron density in the atmosphere below the PMSE layer, so that the transmitted heater power is absorbed in these lower layers. On this day the D-region, as given by the UHF (933 MHz) observations, extends deeper down in the atmosphere than on the other two days, indicating that the degree of ionization in and below the PMSE layers is higher as well.

Keywords. Atmospheric composition and structure (Aerosols and particles; Middle atmosphere – composition and chemistry; Active experiments)

1 Introduction

Artificial electron heating by high power transmitters in the 3–7 MHz range (Rietveld et al., 1993) has been shown to have an effect on atmospheric phenomena, such as auroral emission and airglow (Jones et al., 1986; Kosch et al., 2000), and on the radar phenomenon Polar Mesospheric Summer Echoes (PMSE) (Chilson et al., 2000; Belova et al., 2003). The transmitted heating wave accelerates and heats electrons while the neutrals and ions are unaffected. The weakening of the PMSE, first observed by Chilson et al. (2000), is most likely because the heating of the electrons smooths out the dust-controlled electron density gradients (Rapp and Lübken, 2000, 2003), which are thought to be responsible for the PMSE radar scattering. More recently, it has been discovered (Havnes et al., 2003) that a special use of heater cycling can lead to a new effect where the PMSE can be strengthened. In this heater cycling one first observes a weakening of the PMSE when the heater is switched on, as observed before, and then an increased PMSE strength, compared to the value before the heater was switched on, as the heater is switched off. This effect was predicted (Havnes, 2004) and is called the PMSE overshoot effect. This effect occurs because a density irregularity of charged dust particles will influence the local plasma density in a way which is dependent on the charge density of the dust and on the plasma temperature (Havnes et al., 1984, 1990). For negatively charged

Correspondence to: O. Havnes
(oha003@asp.uit.no)

dust there will be a depletion of electrons inside a dust clump where the dust density is higher than in the near surroundings. When the electron gas is heated the influence of the dust on the electrons is reduced and the depletion is partially filled in. This reduces the local electron density gradient and therefore the radar reflectivity as well. Since the heater is on, the heated electrons will charge the dust particles more negatively. As a result, they regain some of the control over the electrons during the heating-on phase resulting in some recovery of the PMSE signal. When the heater is switched off and the electron temperature nearly immediately returns to its preheating value, equal to that of the ions and neutrals, the increased charges on the dust now force the electrons into a stronger internal depletion than before heating. This also increases the electron gradient and the PMSE strength. The special heater cycling which was used to produce the overshoot was with the heater turned on for 20 s and thereafter turned off for 160 s, to give the PMSE dusty plasma (charged dust/aerosols, ions, electrons) sufficient time to relax back to a state which is unaffected by the heater. With the original heater cycling with ,for example, 20 s on and 20 s off (e.g. Chilson et al., 2000) the dusty plasma would not have enough time to relax completely, so that the dust charges and will become more negative when the heater is on, whithout decharging fully during the short heater-off time. Their charges will therefore be "pumped up" to a steady-state value where the increase during heating equals the reduction during the heating-off time. Havnes (2004) demonstrates that this will lead to a situation where there is no overshoot but where the PMSE returns approximately to its pre-heater value as the heater is switched off. This is what was observed by Chilson et al. (2000) and Belova et al. (2003).

Modelling of PMSE and overshoot (Havnes et al., 2004; Biebricher et al., 2005), assuming that the scattering of radar waves are from electron gradients, which are controlled by dust density gradients (Havnes et al., 1984, 1990; Lie–Svendsen et al., 2003), show that the shape of the overshoot curves vary significantly with the physical conditions in the PMSE region and with the heated electron temperature used in the models. The shape of the overshoot curve will therefore contain information on the PMSE dusty plasma conditions and on the amount of electron heating. In this paper we will examine to what extent the observed electron heating, which can be calculated from the overshoot curves (Havnes et al., 2004; Biebricher et al. 2005), can give information on the electron density. We will, in particular, investigate the effect that electron bite-outs, which are local reductions of electron densities in the height range 80–90 km, can have on the electron heating. Electron bite-outs are caused by concentrations of dust particles within the PMSE layer, which have a high enough density so that they significantly reduce the local electron density by plasma absorption (Pedersen et al., 1969; Ulwick et al., 1988; Havnes et al., 1996a). Since the electron density is also one of the main factors in determining the electron heating, a bite-out may affect the heating sufficiently to influence the PMSE overshoot profiles at different heights. We will also see if the temperature increase factor, $T_{e,\mathrm{hot}}/T_i$, as determined by the overshoot curves, can be used, together with electron heating calculations, to identify if bite-outs are present or not. This, in turn, can assist one in the interpretation of the overshoot curves, to determine the dusty plasma conditions, for example, by telling us if we have a PMSE with a sufficiently high dust density, so that absorption of plasma by dust is important.

In Sect. 2 we briefly describe the theory for artificial electron heating in the lower ionosphere. We show that the electron density profile with electron bite-outs can considerably affects artificial electron heating. We also discuss the importance of the electron density, below the PMSE layer, for the heating in this layer and how the comparatively low heating temperatures which we observe, sometimes with no heating, can result.

In Sect. 3 we will describe the physical background for the model we have adopted for the PMSE overshoot, and show how the adopted model can give the heating factor $T_{e,\mathrm{hot}}/T_i$, by which the electron temperature is heated, relative to the unheated electron temperature T_e, which is identical to the neutral and ion temperatures T_N and T_i. In Sect. 4 some results are presented from a large overshoot campaign which took place at the European Incoherent Scattering (EISCAT) site near Tromsø, Norway in July 2004, with the participation of EISCAT, Germany, Norway, Sweden and UK (Havnes et al., 2006). We will look at selected cases to demonstrate the effect of the electron heating, and we will extract the factor by which the electrons are heated at the different heights according to our PMSE overshoot model. We will further use this to see if the presence of electron bite-outs can be determined.

2 Heating of the middle atmosphere and the effect of electron bite-outs

Heating calculations for different conditions in the middle atmosphere have earlier been presented by Belova et al. (1995) and Kero et al. (2000)among others. We will here just briefly treat the theory for this heating and refer to the above works for more details on this topic.

The heater is transmitting at a frequency f with an effective radiative power ERP. The ERP corresponds to the effect which would have been needed if the transmitter emitted radiation at all 4π solid angles with the same power as it now emits within its beam. In our calculated cases, we have used mainly f=5 MHz, ERP=700 MW and the X mode for the wave. These values are similar to those used in the EISCAT heating campaigns to produce and study the PMSE overshoot phenomenon (Havnes et al., 2003, 2005).

At a certain height the intensity of the wave is I. If no absorption of the wave power has occurred at a height r_0, which we set at 10 km, where we begin the calculation of the propagation with energy loss, we have that $I(10\mathrm{km})=\mathrm{ERP}/4\pi r_0^2$.

The wave energy as a function of height h is now given by a solution of

$$\frac{dI}{dh} = -2kI, \tag{1}$$

where k is the absorption coefficient which is found from the index of refraction n by

$$k = -\frac{\omega Im(n)}{c}. \tag{2}$$

The index of refraction is derived from the Appleton–Hartree theory and depends on electron density, wave frequency and mode, electron collision frequency with neutrals and to a lesser degree on the Earth's magnetic field and propagation direction relative to it. At any height, the enhanced electron temperature is found from a balance between energy input and loss, both being a function of the electron temperature. This is justified by the very short time ($\sim$ a few tens of ms) for the heated electrons to reach their equilibrium temperature. The equation for locally enhanced electron temperature is then

$$2k(T_e)I = L, \tag{3}$$

where the left-hand side is the energy input (Eq. (1)) from the heater and L is the loss function due to elastic collisions of electrons with N_2, O_2 and O (Pavlov, 1998a, b; Pavlov and Berrington, 1999; Jones et al., 2003). The density of the neutral species N_2, O_2 and O, respectively, are taken from the MSIS–E–90 Atmosphere Model (Hedin, 1991).

For the electron densities when unaffected by dust layers, we use the equation

$$\begin{aligned} n_e(h) &= N_e(h_0) && h \geq h_0 \\ n_e(h) &= N_e(h_0)\exp\left(\frac{h-h_0}{H}\right) && h < h_0. \end{aligned} \tag{4}$$

In our calculated cases we have used h_0=90 km and for the scale height H=6 km.

For three different electron density profiles we have calculated the enhanced electron temperature profile for two different values of ERP=600 and 700 MW and show the results in Fig. 1. The higher enhancement of T_e corresponds, naturally, to the larger value of ERP. The maximum ERP of the EISCAT heating facility is estimated to be $\sim$650$\pm$50 MW (private communication, M. T. Rietveld, 2005). The electron temperature in the PMSE region between 80 and 90 km is critically dependent on the electron content in the atmosphere below the PMSE heights. We see this clearly from Fig. 1B which shows the intensity of the heater wave as a function of height for the different cases. The absorption of the heater wave occurs at a low height if n_e is high and much higher up if n_e is low. We also see that the height of maximum absorption approximately coincides with that of the maximum of enhanced electron temperature. Because of the high neutral density at low heights, the energy loss of electrons, due to collisions with neutrals, is then large, and the amplitude of the electron temperature enhancement

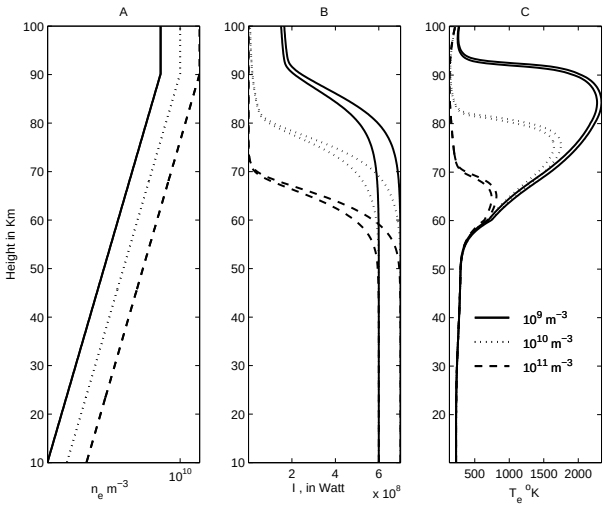

Fig. 1. The heated electron temperature $T_{e,\mathrm{hot}}$ as a function of height for different smooth electron density height profiles (Eq. (4)) is shown in **(C)**. The electron density **(A)** is given by Eq. (4), and n_e at height 90 km is given in the legend. The scale height is H = 6 km. We have used a heater frequency f=5 MHz. Two values for the ERP=600 and 700 MW have been used, with the higher heating corresponding to ERP=700 MW. The intensity of the heater wave as a function of height is given in **(B)**.

is therefore moderate, as shown in Fig. 1C. For absorption at higher altitudes the electron temperature enhancement will be considerably larger. The most effective electron heating occurring at PMSE altitudes is for the model profile with the lowest electron density (solid curve). In Fig. 2 we show the effect on the heated temperature profile from electron bite-outs of various strengths. We see that the general effect of a bite-out is to increase the temperature within and above it (Fig. 2C), compared to a temperature profile without a bite-out, where the electron density follows the profiles given by Eq. (4). For strong bite-outs the heated temperature inside the bite- out can increase slightly with height and be higher than at the bottom of the bite-out. Above the bite-out the temperature will again be decreasing but at temperatures higher than the values that would have resulted without a bite-out. The reason why the bite-out causes a higher temperature than an identical case without a bite-out is shown in Fig. 2B. The reduced electron density within the bite-out leads to a reduced absorption of the heating wave, since the absorption coefficient k decreases with decreasing n_e. Within a strong electron bite-out there is little heater wave absorption. This means that the value of I is higher within and above the bite-out, compared to the case without the bite-out, and this leads to a higher $T_{e,\mathrm{hot}}$ as well.

3 The electron heating as deduced from the overshoot characteristic curve

The overshoot is modelled as the partial reflection of the radar signal from many electron gradients in the PMSE

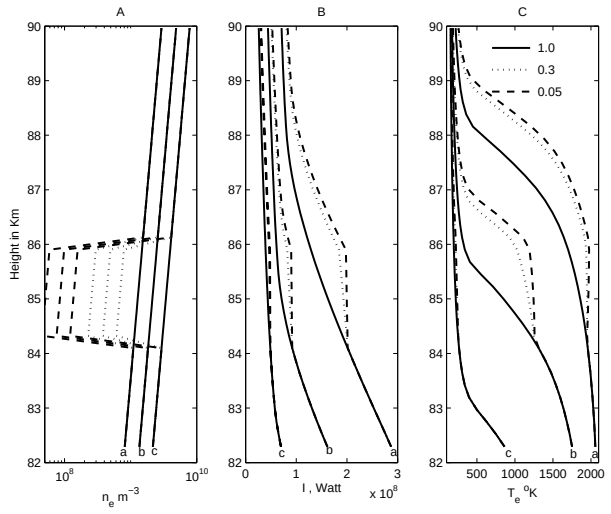

Fig. 2. The heated electron temperatures $T_{e,\mathrm{hot}}$ when an electron bite-out is present in the PMSE region, so that the electron density is locally reduced, are shown in C for three different electron densities (A), given by Eq. (4). The cases **(A)**, **(B)** and **(C)** have an electron density at h=90 km of 3×10^9, 5×10^9 and 8×10^9 m^{-3}, respectively, while H=6 km for all cases. In the bite-outs, which we have placed between 84 and 86 km, the electron densities are reduced with factors 0.3 and 0.05, and we have also shown the cases without bite-outs, i.e. with factor 1; ERP=700 MW. The intensity of the heater wave for the different cases is shown in Fig. B.

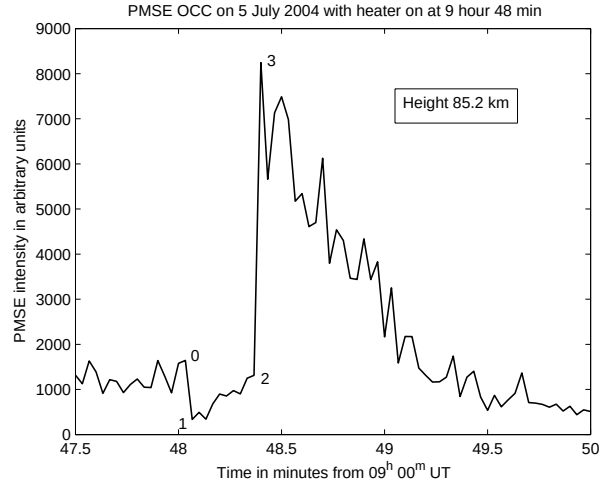

Fig. 3. An example of an observed overshoot characteristic curve (OCC) showing the different phases 0 to 3. The last data point before and the first data point after the heater is switched on is at phase 0 and 1, respectively. The last data point in the heater on phase is 2 and the first data point after the heater is switched off is at 3 after which the dusty plasma and the overshoot relaxes back to their undisturbed value. The observed overshoot shown here, has a shape which is typical for our modelled overshoot curves.

region. These gradients are caused and are controlled by charged dust density irregularities. A concentration of charged dust will influence the ion and electron density, so that if the dust is charged negatively, there will be a depletion of electrons and an increase of ions inside the dust concentration, compared to the values outside it. As long as the dust concentration or clumping exists and the dust particles are charged, the effect on the ion and electron density will be present (Havnes et al., 1984, 1990, 2003; Lie–Svendsen et al., 2003). If the photoelectric effect is not important for dust charging, the dust particles and the dust clumps will be charged negatively. The electrostatic force from the clump will therefore push out some electrons and attract ions. In equilibrium, as in the model used by Havnes et al. (2004) and Biebricher et al. (2005) for the overshoot, the ion and electron densities are given by the Boltzmann relation

$$n_\alpha = n_{\alpha 0} \exp\left(-\frac{q_\alpha V}{k_B T_\alpha}\right), \qquad \alpha = i, e, \tag{5}$$

where q_α is the electron or ion charges. This shows that compared to the average values $n_{\alpha 0}$, there will be a depletion of electrons and an increase of ions inside the clump where $V<0$, where V is the local plasma potential relative to the average plasma potential in the PMSE region, sampled by the radar, which we set to V_0=0. In Eq. (5) the average ion and electron densities, n_{i0} and n_{e0}, will be affected by the average density of dust which is present. In an equilibrium process where ion–electron pairs are produced at a rate q, this will be balanced by a loss due to ion–electron recombination and absorption by dust particles (e.g. Havnes et al., 1992; Rapp and Lübken, 2001). The production rate q can vary between wide limits according to whether we have day or night conditions and/or quiet or disturbed conditions. Rapp (2000) quotes values up to 6300 cm^{-3} s^{-1}. If the dust density is low, we will have $n_{e0}\sim n_{i0}$ and $n_{e0}=(q/\alpha)^{1/2}$, where $\alpha\sim4\cdot10^{-12}$ m^3 s (Brasseur and Solomon, 1995) is the ion–electron recombination coefficient. At a higher dust density n_{e0} and n_{i0} will both decrease, compared to the case with little or no dust, because of the added absorption of plasma by the dust. Inside a dust clump the local values of n_e and n_i will still follow Eq. (5). Since dust charges negatively, the equilibrium situation will be one where the average value $n_{e0}<n_{i0}$, as follows from the quasi-neutrality condition

$$-n_e + n_i + n_d Z_d = 0. \tag{6}$$

Ions are here taken to be singly ionized, and the dust density and charge number is n_d and Z_d, respectively.

As the heater is switched on, the electron temperature in the PMSE region, within a few ten milliseconds, increases to $T_{e,\mathrm{hot}}$ which, in principle, can have a value up to a few thousands °K, if the electron density below the PMSE layers is low so that a large fraction of the transmitted heater energy can propagate to the PMSE heights. The ion and neutral temperatures T_i=T_N are not visibly affected.

In Fig. 3 we show a "classical" example of an observed overshoot curve. The first event is where the PMSE drops rapidly from point 0 to 1 as the heater is switched on. The rest of the phases, also shown in Fig. 3, are the phase from 1 to 2 where the heater is on, then normally an overshoot

phase from 2 to 3 (if the dust density is not too high) when the heater is switched off, and a relaxation phase from 3, to point 0 in the next heater cycle. We assume that as the heater is switched on and the electron temperature increases, the ion and electron density adjustment as a result happens sufficiently rapidly, so that the average plasma density n_{e0} and n_{i0}, and dust charges $Z_d e$, are not affected as the PMSE jumps from point 0 to 1. These parameters can be affected in the phase from 1 to 2, and thereby influence the total overshoot curve, as discussed by Biebricher et al. (2005).

We will approximate a typical radar reflecting an electron density profile, before the heating is switched on, as a linear profile from its centre, with density $n_{e,c}$ to its edge with density n_{e0}, which we have chosen to be equal to the average electron density n_{e0}. The centre densities are described by Eq. (5) with the temperature T_e=T_i at phase 0 in Fig. 3 and T_e=$T_{e,\mathrm{hot}}$ at phase 1. The corresponding normalized potentials at the centre are $\widehat{V}(\mathrm{ph})X(\mathrm{ph})$, where

$$\widehat{V}(ph) = \frac{eV(ph)}{k_B T_i}, \qquad ph = 0, 1 \tag{7}$$

and

$$X(\mathrm{ph}) = \frac{T_i}{T_{e,(\mathrm{ph})}}. \tag{8}$$

Using a reflection coefficient which is proportional to the electron gradient squared (Ginsburg, 1964) we write the ratio of the PMSE strength at phase 1 to that of phase 0 as

$$\frac{R(1)}{R(0)} \approx \left(\frac{n_{e,c}(1) - n_{e0}}{n_{e,c}(0) - n_{e0}}\right)^2. \tag{9}$$

We approximate the electron and ion densities, given by Eq. (5), as a series expansion

$$n_{e,c}(\mathrm{ph}) \approx n_{e0}\left(1 + X(\mathrm{ph})\hat{V}(\mathrm{ph})\right), \tag{10}$$

$$n_{i,c}(\mathrm{ph}) \approx n_{i0}\left(1 - \hat{V}(\mathrm{ph})\right), \tag{11}$$

where the phase ph is 0 or 1. Using Eqs. (10) and (11) in Eq. (6) for phase 0 and 1, we can eliminate $N_d Z$, which does not change from phase 0 to 1, and find the ratio

$$\frac{\hat{V}(1)}{\hat{V}(0)} \approx \frac{n_{e0} + n_{i0}}{X(1)n_{e0} + n_{i0}}. \tag{12}$$

Using Eqs. (12) and (10) in Eq. (9) we find

$$\frac{R(1)}{R(0)} \approx X^2(1)\left(\frac{1 + \frac{n_{i0}}{n_{e0}}}{X + \frac{n_{i0}}{n_{e0}}}\right)^2 \tag{13}$$

which we can solve for the heated electron temperature to find

$$T_{e,\mathrm{hot}} \approx T_i\left(\frac{1 + \frac{n_{i0}}{n_{e0}} - \sqrt{\frac{R(1)}{R(0)}}}{\frac{n_{i0}}{n_{e0}}\sqrt{\frac{R(1)}{R(0)}}}\right). \tag{14}$$

For comparatively low dust densities $n_{i0}/n_{e0}\approx$1 and Eq. (14) gives the upper limit of electron heating as

$$T_{e,\mathrm{hot}} \approx T_i\left(\frac{2 - \sqrt{\frac{R(1)}{R(0)}}}{\sqrt{\frac{R(1)}{R(0)}}}\right). \tag{15}$$

As discussed by Havnes et al. (2003) such situations should be common. On the other hand, situations will certainly occur where the dust density is high and the electron density is correspondingly low, with a presence of electron bite-outs (Pedersen et al., 1969; Ulwick et al., 1988). However, we must also be aware that for very low values of n_{e0} the PMSE strength should, according to our model, be low or absent, since few electrons are present to backscatter (Havnes et al., 1996a; Blix et al., 2003).

A lower limit to the estimated heated temperature $T_{e,\mathrm{hot}}$ is found from Eq. (14) by letting $n_{i0}/n_{e0}\gg$1, which applied for high relative dust densities, if the dust charges are negative, whereby

$$T_{e,\mathrm{hot}} \approx \frac{T_i}{\sqrt{\frac{R(1)}{R(0)}}}. \tag{16}$$

The increase in electron temperature at one height can now be estimated by measuring, at that height, the ratio $R(1)/R(0)$, or the ratio of the PMSE intensity just after the heater was switched on, to the intensity just before it was switched on. Equations (15) and (16) then give the upper and lower limits to the heated electron temperature. However, since a low n_{e0}, and corresponding high n_{i0}/n_{e0} should result in a weak or non-detectable PMSE, we will probably, for observable PMSE, for most cases, be well above the lower limit given by Eq. (16).

It is of interest to find the error if we need to include higher order terms in Eqs. (10) and (11). This will require that the dust charge density $n_d Z_d$, on a length scale comparable to half the radar wavelength λ, changes by a large factor. In such cases the variation in $\widehat{V}$ may not be much less than 1, as we have assumed in Eqs. (10) and (11). For structures comparable to λ (224 MHz) this probably happens very rarely, if at all, as judged from rocket in-situ observations of $n_d Z_d$ as a function of height (e.g. Havnes et al., 1996a, 2001a). However, Havnes et al. (1996b) found a few cases where $n_d Z_d$ varies from $\approx -5\times10^{-9}\,\mathrm{m}^{-3}$ to $-2\times10^{-9}\,\mathrm{m}^{-3}$ over a length of $\sim$3 m. In such cases second order terms of $\widehat{V}$ may be required. Since the electron density in this case is very low, due to the high dust density (Havnes et al., 1996a; Blix et al., 2003), we have $n_{e0}\ll n_{i0}$ and that $\widehat{V}(1)\simeq\widehat{V}(0)$ since few electrons are redistributed when the electron temperature increases (see also Eq. (12)). We further assume that $\widehat{V}(1)\cdot X\ll$1, so that we can linearize for the electron density at phase 1. For the electrons at phase 0 we also include the second order term in the expansion. This gives from Eq. (9) that

$$T_{e,\mathrm{hot}} \approx T_i\,\frac{(1 - \widehat{V}(0)/2)}{\sqrt{\frac{R(1)}{R(0)}}}. \tag{17}$$

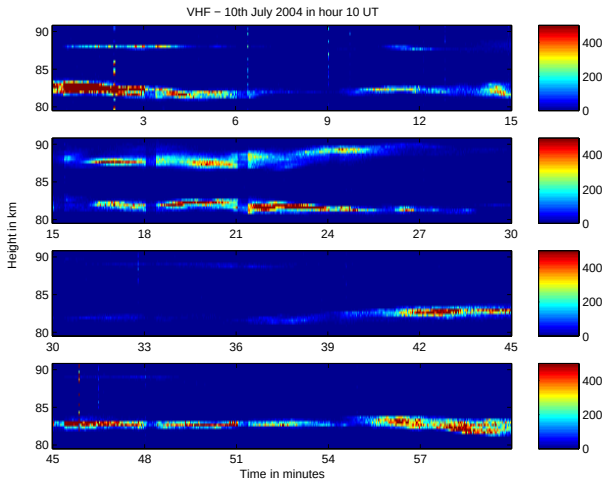

Fig. 4. One hour of raw data of PMSE during one hour on 10 July 2004. In this case the heater transmitter power is at full power on the heater cycles starting at 0 m, 15 m, 30 m and 45 m while it is reduced in steps of 20% of the full power, at each subsequent heater cycle, down to 20% of full power and then returned to full power.

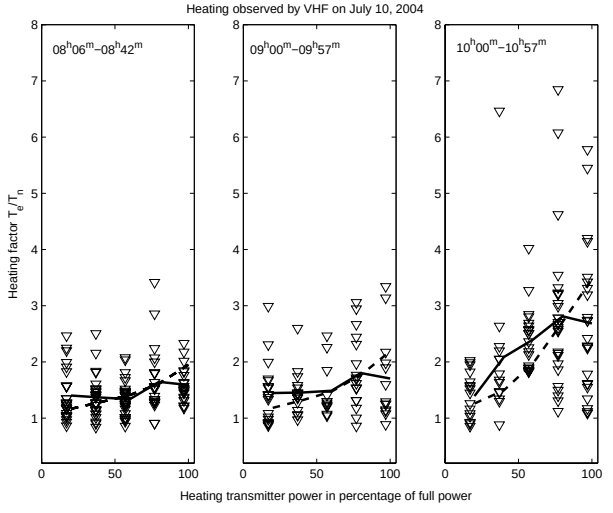

Fig. 5. All calculated heating factors $T_{e,\mathrm{hot}}/T_i$, for three hours of observations, plotted against the transmitter power in percent of full power. The full line shows the line through the average of the observed heating factors for the different heater transmitter intensities, while the dotted lines are the average heating, over the height interval 81–89 km, resulting from model calculations shown in Fig. 6, see text.

Since $\widehat{V}(0)$ is negative and of the order of 1 this will be comparable to the results of Eq. (15) for reasonable heating factors. This also shows that the lower limit (Eq. (16)) for the high density cases will be increased when non linear terms are included.

4 Electron heating as observed from overshoot curves

In Fig. 4 we show the results of one-hour observations by the EISCAT VHF (224 MHz) radar during an international overshoot campaign in July 2004 (Havnes et al., 2005). The radar was run with the EISCAT arc-dlayer program with integration time 0.2 s. The heater was in all the cases we consider here, run at frequency 5.234 MHz, in the X-mode. Figure 4 shows a one-hour observation where the heating power was modulated in several steps. The heating cycle was started at a full hour with maximum ERP of 650±50 MW, thereafter the power was reduced in steps of 20% down to 20% of full power, then the whole pattern was repeated. Each power step lasted 3 min during which the heater was switched on for the first 20 s and was off for 160 s. Since a whole power cycle lasts 15 min, the full power will be at 0 min, 15 min, 30 min and 45 min of each full hour. Although the PMSE strength varies strongly during this one-hour interval, we see the clear effect of the heater in most of the 3-min cycles. The strength of PMSE is reduced during 20 s when the heater was on, often followed by the overshoot when the heater was switched off. The heating effect weakens as the transmitter power is reduced. At 20% the effect is weak but it is still observable at some heights. This scheme of heater power reductions was used as a test to see if our model for temperature increase would show clear effects of the power reductions. In Fig. 5c we show the temperature increase factor $1/X = T_{e,\mathrm{hot}}/T_i$ for all 3-min cycles of Fig. 4 and all heights for which the PMSE is present. In Fig. 5a and b we show the same for the two hours preceding that of Fig. 4. The values are plotted against the heater transmitter power, given in percent of full power.

We see from Figs. 5a,b and c that the average temperature increase factors (shown as full lines), in general, show a decrease with decreasing heater transmitter power and that it also is different for the three hours 08:00–09:00, 09:00–10:00 and 10:00–11:00 UT. While heating is strong and easily seen in Figs. 4 and 5c, it is weak or absent for the two hours of observing from 08:00–10:00 UT. This indicates that the physical condition changed during these three hours. While the main absorption of the heating wave must be well below the PMSE layer in the cases of Figs. 5a and b, it should be lifted to occur in the lower part of the layer during most of the hour from 10:00-11:00 UT in Fig. 5c. In Fig. 6a and b we show calculated examples of heating as a function of height, with the heater power varied from 100% in steps of 20% down to 20%. The electron density is taken to vary as in Eq. (4). The highest electron density case in Fig. 6a represents fairly well the averaged results of hour 08:00–09:00 UT in Fig. 5a while those of Fig. 6b could represent the case in Fig. 5c. In Figs. 5a and c we show, as a broken line, the heating factors from Figs. 6a and b, respectively, averaged (for a fixed heater power) over all heights from 81 to 89 km, which is roughly the height region within which the PMSE was observed for these cases. The dotted line in Fig. 5b corresponds to calculated cases with $N_e = 8.5\times10^9\ \mathrm{m}^{-3}$.

We should be aware that each of the Figs. 5a, b and c represents one hour of observation and shows the heating

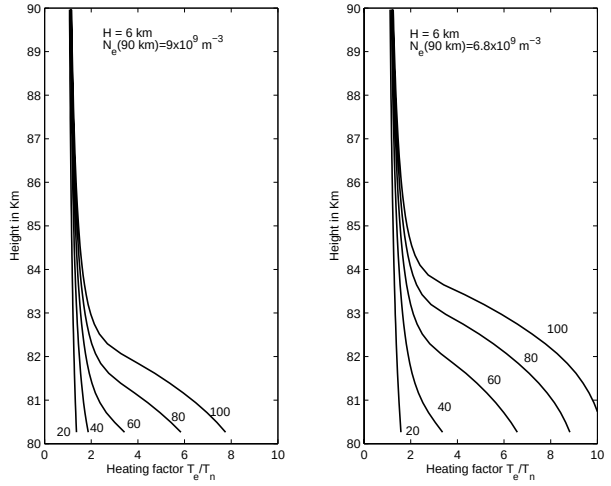

Fig. 6. The change of heating, for two electron density profiles, as the heater transmitter power is changed from full power (100) in steps of 20% down to 20% of full power (20). The left-hand cases, with the highest electron density profile, are taken to represent the case 08:00–09:00 UT in Fig. 5, where the average heating factor between 81–89 km is shown as a broken line. The lowest electron density profile on the right is taken to represent the case for 10:00–11:00 UT in Fig. 5. ERP=700 MW.

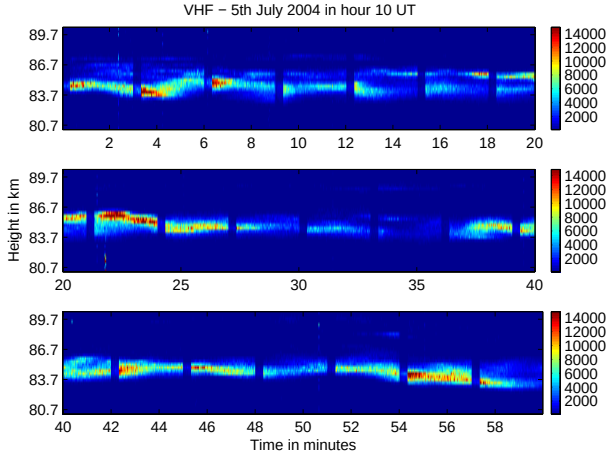

Fig. 7. One hour of raw data. The heater transmitter is now run at full power in all cycles. The overshoot cycles are each 3m long and the heater is on for 20 s. This is clearly shown as a reduced intensity with 3m interval, lasting for 20 s, followed in most cases by strong overshoots.

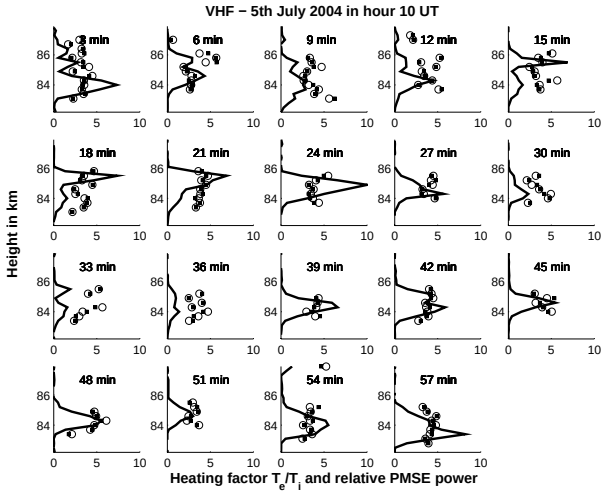

Fig. 8. Here we show the heating factor as a function of height for each of the 19 overshoot cycles in the one hour of observations shown in Fig. 6. The PMSE relative height power profiles, normalized to an arbitrary value of 10 for the largest value, are also shown. The filled squares are the results when the PMSE intensities at points 0 and 1 (Fig. 3) are found from a best fit second-order polynomial through the 10 s before or after the heater is switched on. The open circles are the results from using the 2-s integrated values at point 0 and at point 1.

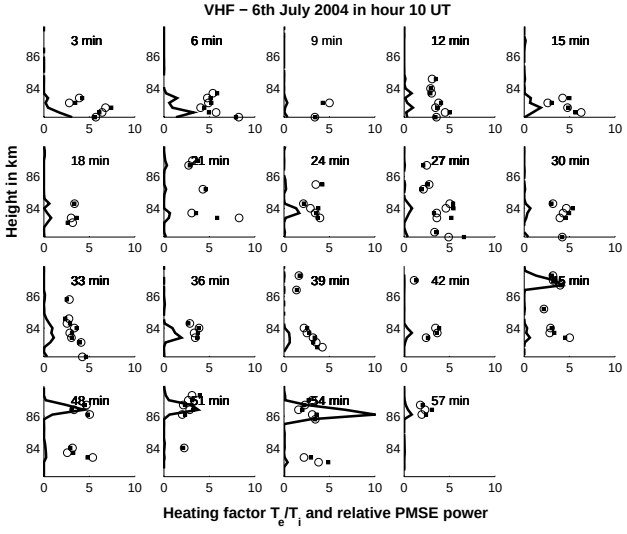

Fig. 9. As in Fig. 8, but now for hour 10:00 UT on 6 July 2004.

factor $T_{e,\mathrm{hot}}/T_i$ for all heights where PMSE is observed. The scatter is therefore necessarily large, and the results mainly demonstrate that there is a general decrease in the heating as calculated by Eq. (15), when the heater power is reduced. Besides natural variations of the heating factor due to variations in the dusty plasma conditions, there will be an uncertainty in the values of the intensities $R(0)$ and $R(1)$ (Eq. (9)) due to the rapid variations in the signal. We have calculated $T_{e,\mathrm{hot}}/T_i$ based on the values of $R(1)$ and $R(0)$, as given by the 2-s sampling just before and after the heater was switched on. We call this the direct value method. We have also calculated $T_{e,\mathrm{hot}}/T_i$ when $R(0)$ is found by a best fit of a second-order polynomial to the 10 s of data before the heater is switched on, and $R(1)$ for the 10 s data after the heater is switched on. We call this the smoothed value method. The results of the heating factor calculated by these two methods is shown directly in Figs. 8, 9 and 10. Although the difference is generally comparatively small, the standard deviation

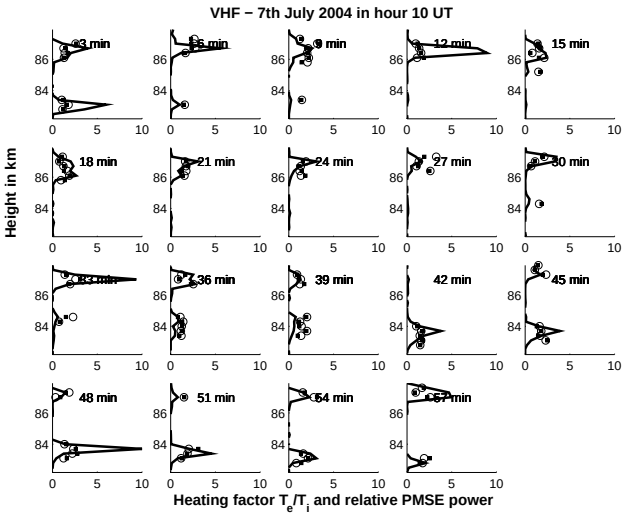

Fig. 10. As in Fig. 8, but now for the hour 10:00 UT on 7 July 2004.

of the difference between the two methods for the heating factor is 0.2 for Figs. 5a and b. This also supports that the relatively modest deviations of the average PMSE strength, as a function of transmitter power, from the smoothly decreasing model curve, is probably not significant. Also, the change in conditions, which leads to higher heating in the hour 10:00–11:00 UT, most likely does not change abruptly and the low heating of hour 09:00–10:00 UT may well have extended into the following hour. If we look at Fig. 4 this appears to be the case since the first heating cycles, in the first power cycle (0–15 min), which show little weakening compared to those of the next power cycle (15–30 min). In fact, for the case of Fig. 5c, if we excluded the first power cycle of 100% ERP, the main result is that the average value at 100% power is raised from its present value of ∼2.7 to ∼3.2. This removes completely the anomalous behaviour in Fig. 5c, where the average heating factor increases slightly when going from 100% to 80% of full power, and shows the expected decrease in heating as the heating power is reduced. We take the general agreement between the calculated and observed heating variations as an indication that our model for the PMSE overshoot, although without doubt not the final answer, is, in its basic concept, correct.

In Figs. 7 to 10 we show the results from one-hour observations on each of the three consecutive days. The heater is now run on full power when switched on, and we use a cycle with the heater on for 20 s and off for 160 s. In Fig. 7 we see the raw data for one hour, starting at 10:00 UT on 5 July 2004. In Fig. 8 we show the measured electron temperature increase factor of $1/X$ by the direct (black squares) and smoothed value method (open circles) for all the heater cycles of that hour, together with the normalized height profile (continuous line) of the PMSE just before the heater was switched on. The normalization is such that the largest value of the PMSE just before the heater is switched on is set at 10 and the other curves are scaled according to this. We see that the largest value is for the cycle starting at 24 min, which agrees with Fig. 7.

In Figs. 9 and 10 we show the electron temperature increase factor of $1/X$, also computed by both methods, and the scaled PMSE height profiles, for hour 10:00 UT on 6 and 7 July 2004, respectively. In Figs. 8 to 10 the temperature increase factor is plotted only if the backscatter signal is larger than two times the standard deviation of the background signal without PMSE. The heating cycle is again 20 s on and 160 s off. We see that there is a clear difference between the heating factor of $1/X$ for the three days. From the theoretical heating curves (e.g. Fig. 6), the heating factor should decrease smoothly, if the peak is below the PMSE, which is probably the case in all our observations. In Fig. 8 for 5 July we very often see a $1/X$ heating factor variation with an increase in heating with height, indicating the presence of an extended bite-out over a few km, from approximately 84 to 86 km. On 6 July, in Fig. 9, although there is considerable scatter, we most often see a tendency for $1/X$ to decrease with height. This indicates that the absorption of plasma by the dust is small to moderate and that bite-outs are generally absent, except probably during the last five cycles, where a comparatively strong PMSE suddenly appears at 86.5 km and where $1/X$ increases with height. This is most likely caused by an electron bite-out. For 7 July, in Fig. 10, we have a case with little or no heating, since we see that generally $1/X \sim 1$ to 2. This should be a result of a higher electron density below the PMSE layer than on the 5 and 6 July, resulting in a transmitter power that is now nearly fully absorbed lower down, as demonstrated earlier (Belova et al., 1995; Kero et al., 2000) and shown in Figs. 1 and 6.

For 5 July, where bite-outs should be present, the PMSE layer is appearing at about 07:00 UT and increases gradually to become its strongest and widest toward the end of the observing period between ≈09:30–11:00 UT. On our arbitrary scale the maximum PMSE power, just before the heater is switched on, is ∼12 000 during the one hour from 10:00–11:00 UT. For the same hour on 6 July the power is $\lesssim$700–800 until the sudden appearance of the layer at ∼86.5 km height at time ∼10:45 which reaches a maximum of ∼3000. This is consistent with our earlier findings (Havnes et al., 2001a,b) of how the PMSE varies intensity with the amount of dust which is present. In terms of the ratio $P = n_d Z_d / n_{e0}$ they found that the PMSE intensity initially increases rapidly with P, reaches a plateau at $P \sim 0.2$–0.3, which may last until $P \sim 0.5$, decreases towards zero for large P since then a few free electrons will be present to scatter. If the PMSE on 5 and 6 July are on the part where the PMSE intensity increases with P, or on the plateau, the generally stronger PMSE on 5 July should indicate a considerably larger value of P and a correspondingly larger absorption of electrons, a bite-out. The weakness of the heating in the layer on 7 July, with a peak power of about 500, should, as earlier discussed, be a result of a higher electron density below the PMSE layer on this day. This is supported by the height profile of the lower end of the D-layer, as shown in Fig. 11, for the observations with the EISCAT UHF (933 MHz) antenna. On 7 July the

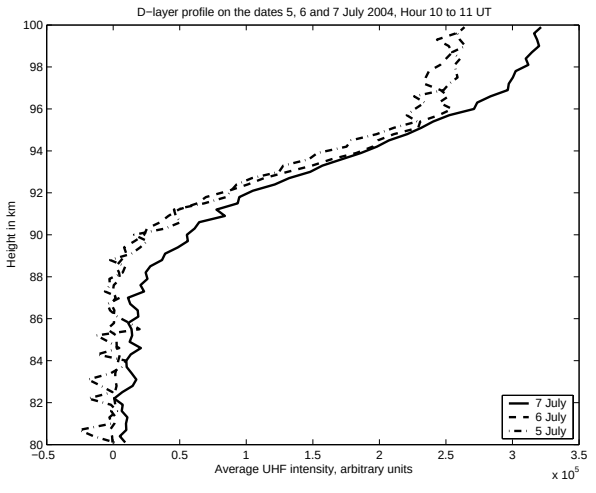

Fig. 11. A plot of the lower part of the D-layer as observed with the EISCAT UHF (933 MHz) radar on the dates 5, 6 and 7 July 2004.

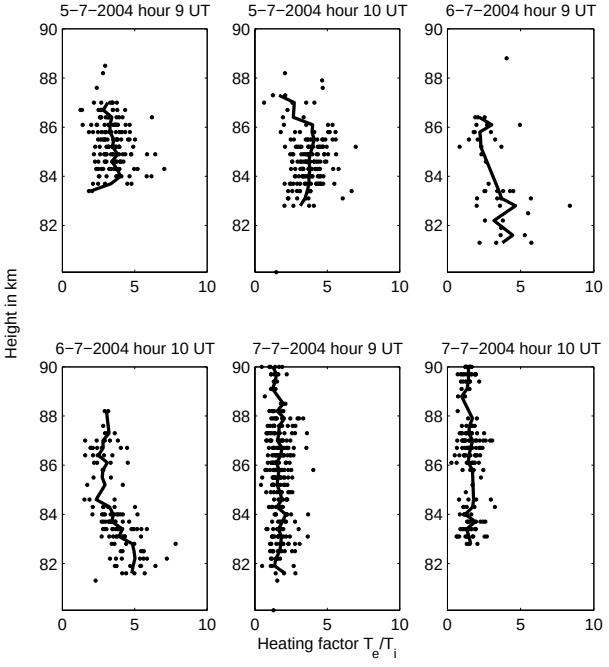

Fig. 12. The heating factors and their averages as a function of height, are plotted for two hours on each of the dates 5, 6 and 7 July 2004.

layer is stronger and extends deeper than on 5 and 6 July, indicating a higher ionization as well.

In Fig. 12 we show the individual heating factors, and their averages, for two hours on each of the days 5, 6 and 7 July 2004. These also confirm our impression from Figs. 8, 9 and 10 that a strong bite-out is present during hour 10:00 UT on 5 July. The comparatively high value of T_e/T_i and its slow decrease with height above ∼84 km during the hour starting at 09:00–00:00 UT indicate that a moderate bite-out is present. On 6 July the behaviour is dominated by a decrease in the heating factor with height for both hours but with a possible bite-out being present, as earlier discussed, around 86.5 km during part of hour 10:00 UT. Both hours for 7 July indicate little or no heating, on average.

5 Conclusion

The model for the PMSE overshoot has been successful in describing the various forms of the overshoots which we observe and the dependence of these shapes on the dusty plasma parameters (Havnes et al., 2003, 2004; Biebricher et al., 2005). This also lends credence to the fact that the overshoot curves can give the temperature increase factor $1/X{=}T_{e,\mathrm{hot}}/T_i$ when the heater transmitter is switched on during PMSE conditions. Support for this is found from the series of observations and comparison with models for heating, Figs. 4 to 6, where the heater transmitter power is changed from cycle to cycle in steps of 20% power, down to 20%, after which the power is returned to 100% and a new sequence of diminishing heater transmitter power is started. As we see from Fig. 4 the effect on the strength of the PMSE is, as expected, reduced as the transmitter power is reduced. The heating factor of $1/X$, as calculated from observations by the use of Eq. (15), also gives reduced heating and Fig. 5 for 10 July shows how this, on the average, follows the reduction in heating transmitter power. We also see from Figs. 8, 9 and 10, that the heating factor, as a function of height, can vary considerably from day to day and also within one day, from one heater cycle to the next. However, on average, there is a systematic difference between the heating effect as a function of height for the different days. Apart from cases where no heating effect is observed, the difference on days where the heating effect is present should be mainly due to differences in the relative amount of dust compared to that of electrons. For a high relative value, electron absorption by dust can then lead to electron bite-outs which will influence the electron heating with height. An uncertainty in the computation of $T_{e,\mathrm{hot}}/T_i$ (Eq. (14)) is that the ratio n_{i0}/n_{e0} is not known. Our results have been taken for cases where this ratio is ≈1. If n_{i0}/n_{e0} is significantly higher than 1, as it would be in an extended bite-out, the resulting heating factor will be lower than what we have found by Eq. (15) and used in Figs. 5, 8, 9 and 10. However, the reduction will not be very large, at the most, if we take the ratio between $T_{e,\mathrm{hot}}$ of Eqs. (15) and of Eq. (16), we see that the maximum reduction, if $\sqrt{R(1)/R(0)}\to 0$, will be by a factor of 2. If we take the value of $\sqrt{R(1)/R(0)}{=}1/3$, which gives a heating factor of $1/X{=}5$ by Eq. (15), we find from Eq. (14) that if $n_{i0}/n_{e0}{=}2$ or 4, the value of $1/X$ will be decreased to 4 and 3.5, respectively. This shows that the results for $1/X$ in Figs. 8 to 11 can only be modified significantly if we accept that a strong electron bite-out is present. Such a modification cannot remove the increase of heating with height but may lower the general level of heating. This also strengthens our findings that we, in our observations of the effects of the heater, have never been near the very high electron heating up

to a few thousands °K which is theoretically possible (Belova et al., 1995) but that our results indicate $T_{e,\mathrm{hot}} \lesssim 1000$°K.

We find the present method, to look for large dust concentrations from the run of the heating factor with height, to be a new and promising tool to investigate the PMSE conditions. Since the dust is so crucial in controlling the PMSE, it is vital to obtain information on the dust content when studying the PMSE phenomenon.

Acknowledgements. The EISCAT Scientific Association is funded by SA (Finland), CNRRS (France), MPG (Germany), NIPR (Japan), RCN (Norway), NFR (Sweden), and PPARC (UK). This research was conducted under grants from the Research Council of Norway. The authors would like to thank L. Larssen for preparing the manuscript. The two referees are thanked for their many and relevant comments which helped improve the paper.

Topical Editor M. Pinnock thanks A. Kero and M. Rapp for their help in evaluating this paper.

References

Belova, E. G., Pashin, A. B., and Lyatsky, W. B.: Passage of powerful HF radio wave through the ionosphere as a function of initial electron density profiles, J. Atmos. Terr. Phys., 57, 265–272, 1995.

Belova, E., Chilson, P. B., Kirkwood, S., and Rietveld, M. T.: The response time of PMSE to ionospheric heating, J. Geophys. Res., 108, 8446, 2003.

Biebricher, A., Havnes, O., Hartquist, T. W., and La Hoz, C.: On the influence of plasma absorption by dust on the PMSE overshoot effect, Adv. Space Res., in press, 2005.

Blix, T. A., Rapp, M., and Lübken, F.-J.: Relations between small scale electron number density fluctuations, radar backscatter, and charged aerosol particles, J. Geophys. Res., 108, D8, 8450, doi:10.1029/2002JD002430, 2003.

Brasseur, G. and Solomon, S.: Aeronomy of the Middle Atmosphere, D. Reidel Publ. Comp., 1995.

Chilson, P. B., Belova, E., Rietveld, M. T., Kirkwood, S., and Hoppe, U.-P.: First artificially induced modulation of PMSE using the EISCAT heating facility, Geophys. Res. Lett., 27, 3801–3804, 2000.

Ginsburg, V. L.: The Propagation of Electromagnetic Waves in Plasmas, Pergamon Press, 1964.

Havnes, O.: Polar Mesospheric Summer Echoes (PMSE) overshoot effect due to cycling of artificial electron heating, J. Geophys. Res., 109, A02309, 2004.

Havnes, O., Morfill, G. E., and Goertz, C. L.: Plasma potential and grain charge in a dust cloud embedded in a plasma, J. Geophys. Res., 89, 10 999–11 003, 1984.

Havnes, O., Aanesen, T. K., and Melandsø, F.: On dust charges and plasma potentials in a dusty plasma with dust size distribution, J. Geophys. Res., 95, 6581–6585, 1990.

Havnes, O., Melandsø, F., La Hoz, C., Aslaksen, T. K., and Hartquist, T.: Charged dust in the Earth's mesopause: Effects on radar backscatter, Phys. Scripta, 45, 535–544, 1992.

Havnes, O., Trøim, J., Blix, T., Mortensen, W., Næsheim, L. I., Thrane, E., and Tønnesen, T.: First detection of charged dust particles in the Earth's mesosphere, J. Geophys. Res., 101, 10 839–10 847, 1996a.

Havnes, O., Næsheim, L. I., Hartquist, T. W., Morfill, G. E., Melandsø, F., Schleicher, B., Trøim, J., Blix, T., and Thrane, E.: Meter-scale variations of charge carried by mesospheric dust, Planet. Space Sci., 44, 1191–1194, 1996b.

Havnes, O., Aslaksen, T., and Brattli, A.: Charged dust in the Earth's middle atmosphere, Phys. Scripta, T89, 133–137, 2001a.

Havnes, O., Brattli, A., Aslaksen, T., Singer, W., Latteck, R., Blix, T., Thrane, E., and Trøim, J.: First common volume observations of layered plasma structures and polar mesospheric summer echoes by rocket and radar, Geophys. Res. Lett., 28, 1419–1422, 2001b.

Havnes, O., La Hoz, C., Næsheim, L. I., and Rietveld, M. T.: First observations of the PMSE overshoot effect and its use for investigating the conditions in the summer mesosphere, Geophys. Res. Lett., 30, 2229, 2003.

Havnes, O., La Hoz, C., Biebricher, A., Kassa, M., Meseret, T., Næsheim, L. I., and Zivkovic, T.: Investigation of the mesospheric PMSE conditions by use of the new overshoot effect, Phys. Scripta, T107, 70–78, 2004.

Havnes, O., La Hoz, C., Aylward, A., Belova, E., Hartquist, T. W., Kosch, M. J., Morfill, G., Næsheim, L. I., Rietveld, M. T., Rubin-Zuzic, M., and Sigernes, F.: The radar PMSE overshoot effect as a diagnostic method, Adv. Space Res., in press, 2006.

Hedin, A. E.: Extension of the MSIS thermosphere model into the middle and lower atmosphere, J. Geophys. Res., 96, 1159–1172, 1991.

Jones, T. B., Robinson, T. R., Stubbe, P., and Kopka, H.: EISCAT observations of the heated ionosphere, J. Atmos. Terr. Phys., 48, 1027–1035, 1986.

Jones, D. B., Campbell, L., Bottema, M. J., and Brunger, M. J.: New electron-energy transfer rates for vibrational excitation of O_2, New J. Phys., 5, 114, 2003.

Kero, A., Bösinger, T., Pollari, P., Turunen, E., and Rietveld, M.: First EISCAT measurements of electron-gas temperature in the artificially heated D-region ionosphere, Ann. Geophys., 18, 1210–1215, 2000,
SRef-ID: 1432-0576/ag/2000-18-1210.

Kosch, M. J., Rietveld, M. T., Hagfors, T., and Leyser, T. B.: High-latitude HF-induced airglow displaced equatorwards of the pump beam, Geophys. Res. Lett., 27, 2817–2820, 2000.

Lie–Svendsen, Ø., Blix, T. A., Hoppe, U.-P., and Thrane, E. V.: Modeling the plasma response to small-scale aerosol particle perturbations in the mesopause region, J. Geophys. Res., 108, 8442–8465, 2003.

Pavlov, A. V.: New electron energy transfer rates for vibrational excitation of N_2, Ann. Geophys., 16, 176–182, 1998a,
SRef-ID: 1432-0576/ag/1998-16-176.

Pavlov, A. V.: New electron energy transfer and cooling rates by excitation of O_2, Ann. Geophys., 16, 1007–1013, 1998b,
SRef-ID: 1432-0576/ag/1998-16-1007.

Pavlov, A. V. and Berrington, K. A.: Cooling rate of thermal electrons by electron impact excitation of fine structure oxygen, Ann. Geophys., 17, 919–924, 1999,
SRef-ID: 1432-0576/ag/1999-17-919.

Pedersen, A., Trøim, J., and Kane, J.: Rocket measurement showing removal of electrons above the mesopause in summer at high latitudes, Planet. Space Sci., 18, 945–947, 1969.

Rapp, M.: Aerosol layers in the polar summer mesosphere: Interaction with the plasma of the D-region and dependence on temperature and dynamics, thesis, Bonn Univ., Bonn, 2000.

Rapp, M. and Lübken, F.-J.: Electron temperature control of PMSE, Geophys. Res. Lett., 27, 3285–3288, 2000.

Rapp, M. and Lübken, F.-J.: Modelling of particle charging in the polar summer mesosphere, 1, General results, J. Atmos. Sol. Terr.

Phys., 63, 759–770, 2001.

Rapp, M. and Lübken, F.-J.: Comment on "The response time of PMSE to ionospheric heating" (Ed.) Belova, E., P. B. Chilson., S. Kirkwood., and T. Rietveld et al., J. Geophys. Res., 108, doi:10.1029/2003JD003638, 2003.

Rietveld, M. T., Kohl, H., and Kopka, H.: Introduction to ionospheric heating at Tromsø 1. Experimental overview, J. Atmos. Terr. Phys., 55, 577–599, 1993.

Ulwick, J. C., Baker, K. D., Kelley, M. C., Balsley, B. B., and Ecklund, W. L.: Comparison of simultaneous MST radar and electron density probe measurements during state, J. Geophys. Res., 93, 6989–7000, 1988.